# CHARACTERIZATION OF THE BALCONES 60 MJ PULSED POWER SUPPLY CIRCUIT PARAMETERS

D. J. Hildenbrand

Presented at the
6th IEEE Pulsed Power Conference
Marriott Crystal Gateway
Arlington, Virginia
June 29-July 1, 1987

Publication No. PN-112
Center for Electromechanics
The University of Texas at Austin
Balcones Research Center
EME 1.100, Building 133
Austin, TX 78758-4497
(512)471-4496

# CHARACTERIZATION OF THE 60 MJ BALCONES HPG POWER SUPPLY CIRCUIT PARAMETERS

D. J. Hildenbrand and R. C. Zowarka, Jr.

Center for Electromechanics
The University of Texas at Austin
Austin, TX 78758-4497

## Summary

The Center for Electromechanics at The University of Texas at Austin is presently working to complete the start-up testing of the 60 Megajoule (MJ) Balcones Homopolar Generator (HPG) Power Supply. Six identical homopolar generators (HPG's) are utilized to produce megamp current pulses for use in industrial welding and electromagnetic launch technologies (900 MW generators alone; 10 GW generators with power conditioning).

An integral part of the start-up is the determination of each generators' electrical circuit impedance. The theoretical premise, test procedures and equipment used to determine the HPG and connecting copper bus circuit parameters of equivalent capacitance (C), inductance (L), and resistance (R) are presented. Consideration is given to the aspects of equivalent capacitance modeling of the HPG. Also discussed are the effects of armature reaction and current magnetic diffusion skin depth on the determination of the values of R, L, and C.

## Introduction

The pulsed power supply consists of six identical HPG's rated at 10 MJ each and suitable for various series and/or parallel electrical connections to provide maximum current ratings from 1.5 MA at 600 Vdc (six series) to 9 MA at 100 Vdc (six parallel).

Each generators output terminals are brought above floor elevation via a pair of 2 x 24 in. copper busbars (referred to as bus risers). Generator loads and or interconnecting bus assemblies are attached at this point. Figure 1 illustrates in cross section the generator, output spider, current compensating turns, and bus riser. Also visible are the generator instrument brushes. These brushes are used to measure the open circuit voltage of the generator prior to connection to the load and to provide a voltage profile of the machine during discharge.

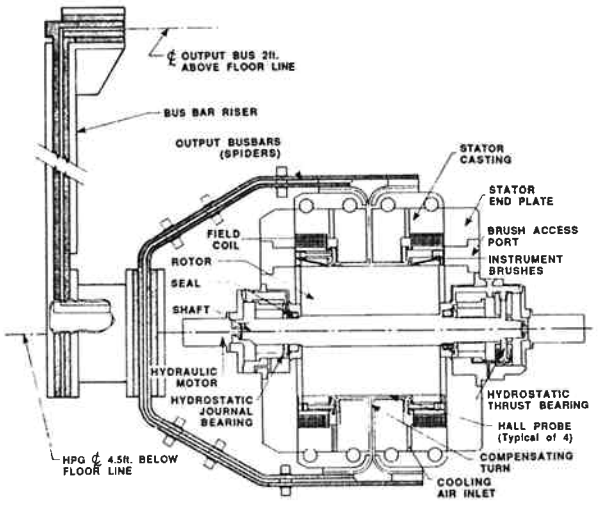


Figure 1. HPG and bus riser cross sectional view

The power supply is suitable for applications ranging from industrial welding to electromagnetic railguns. For this reason the analysis presented herein is constrained to the determination of HPG circuit parameters up to and including the bus riser only. The first load to be used on the system will be the power conditioning inductors for a hypervelocity EM gun test facility. A brief discussion will be presented on the effects of increased values of circuit inductance on time to peak current, armature reaction, and magnetic diffusion skin depth.

For characterization the generator output was terminated into a short circuit load of known inductance and resistance. The generator and bus riser were treated as lumped RLC parameters. Based on predicted values for these parameters an overdamped circuit analysis was utilized. Classical circuit analysis was performed in conjunction with discharge data to arrive at the effective values of R, L, and C. The value of the effective resistance ($R_{eq}$) is conditional upon the assumption of an average sliding contact resistance.

The test procedures and equipment used to determine the circuit parameters have provided accurate results which compare favorably with the theoretical values. The high speed digital recording system used to measure the HPG instrument brush and bus riser voltages, rotor speed, field flux, and discharge current is described herein.

The measurement of system parameters has improved over previous generator tests. These improvements include the addition of instrument brushes which establish the initial conditions of HPG voltage and field flux, a very accurate time resolved speed measurement that allows the time resolution of generator voltage, which in turn allows for the calculation of time varying circuit parameters, the accurate calibration of current measurement systems with a low inductance current viewing resistor (CVR) and the installation of hall effect transducers to resolve the evolution of the generator excitation flux during discharge. These diagnostics will allow the generation of empirical models, verification of theoretical models and ultimately a better understanding of the issues of pulsed power system design, resulting in smaller, more efficient systems.

## Circuit Modeling

An equivalent lumped parameter model has been determined. $R_{eq}$, $C_{eq}$, and $L_{eq}$, as shown in figure 2 are representative of the sum of discrete component values of the respective generator/bus riser current carrying assemblies. The parameter values are based upon the discharge performance levels shown below in table 1.

## Determination of Circuit Parameters-- Classical Analysis

The HPG models electrically as a capacitor. The equivalent capacitance ($C_{eq}$) is found by equating the expressions for the mechanical and electrical stored energies. $C_{eq}$ is found to be independent of rotor

Table 1. Parameter Values

| |
|---|
| Load: 56 μΩ, 225 nH stainless steel loop resistor |
| Results: |
| Peak Current: 120.5 kA at 30 ms |
| Open Circuit Voltage: 9.46 Vdc |
| Open Circuit Rotor Speed: 66 rad/s |
| $R_{eq}$ = 13.7 (± 1.0) μΩ |
| $L_{eq}$ = 432 nH |
| $C_{eq}$ = 2563.82 farads |

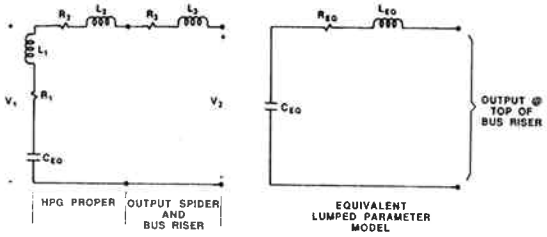


CIRCUIT PARAMETERS:

$R_1$ : ROTOR RESISTANCE
$R_2$ : SLIDING CONTACT & COMPENSATION CIRCUIT RESISTANCE
$R_3$ : OUTPUT SPIDER/BUS RISER RESISTANCE
C : EQUIVALENT HPG CAPACITANCE
$L_1$ : ROTOR INDUCTANCE
$L_2$ : SLIDING CONTACT & COMPENSATION CIRCUIT INDUCTANCE
$L_3$ : OUTPUT SPIDER/BUS RISER RESISTANCE
$V_1$ : INSTRUMENT BRUSH VOLTAGE
$V_2$ : BUS RISER VOLTAGE

Figure 2. Equivalent circuit models

speed (ω) and inversely proportional to the square of the excitation flux (Φ).

Stored Capacitive Energy ($W_C$) = $C_{eq}V_o^2/2$ (joules) (1)

Stored Mechanical Energy ($W_m$) = $J\omega_o^2/2$ (joules) (2)

HPG Terminal Voltage ($V_o$) = $\omega_o\Phi/2\pi$ (volts) (3)

where

$\omega_o$ = predischarge rotor speed in radians/s

By equating $W_C$ and $W_m$ then solving for $C_{eq}$ and substituting (3) for $V_o$ yields:

$$C_{eq} = \frac{4\pi^2 J}{\Phi^2} \quad \text{(farads)} \qquad (4)$$

When determining the actual value for $C_{eq}$ from the test data the value of $W_m$ is found from the predischarge rotor speed ($\omega_o$). Given that the inertia (J) is a constant and the HPG energy rating of 10 MJ at 633 rad/s, $W_m$ at $\omega_o$ can be found by scaling the energies as follows:

$$(W_m \text{ at } 633 \tfrac{\text{rad}}{\text{s}}) \left[\frac{\omega_o}{633}\right]^2 = W_m \text{ at } \omega_o \tfrac{\text{rad}}{\text{s}} \qquad (5)$$

therefore,

$$W_m \text{ at } \omega_o = 10^7 \left[\frac{\omega_o}{633}\right]^2 \qquad (6)$$

from which,

$$C_{eq} = \frac{2 \times 10^7 \left[\frac{\omega_o}{633}\right]^2}{V_o^2} \qquad (7)$$

where $\omega_o$ and $V_o$ can be determined from the discharge data.

Having established an RLC circuit model, then the behavior of current as a function of time should necessarily adhere to the predictions governed by the second order differential equation:

$$L\frac{di}{dt}(t) + \frac{1}{C}\int i(t)dt - V_o(0) + i(t)R = 0 \qquad (8)$$

With the assumption of overdamped response the natural solution will have two real roots with the general form of:

$$i(t) = A_1\exp(S_1 t) + A_2\exp(S_2 t) \qquad (9)$$

where,

$$S_{1,2} = \frac{R}{2L} \pm \sqrt{\left(\frac{R}{2L}\right)^2 - \frac{1}{LC}} \quad , R > 2\sqrt{\frac{L}{C}} \qquad (10)$$

or,

$$S_{1,2} = \alpha \pm \sqrt{\alpha^2 - \omega_r^2} = \alpha \pm \omega_d \qquad (11)$$

then the closed form solution becomes:

$$i(t) = \left(\frac{V_0}{2\omega_d}\right)e^{-\alpha t}\left[e^{+\omega_d t} - e^{-\omega_d t}\right] \text{ (amps)} \qquad (12)$$

By establishing the dimensionless parameter γ1

$$\gamma = \frac{\alpha}{\omega_r} = \frac{R}{2}\sqrt{\frac{C}{L}} \qquad (13)$$

the values of peak current can be determined as a function of time for specific values of γ. Figure 3(1) shows the variations of the normalized value of peak current as a function of normalized time to peak with γ as a parameter.

Normalized values of current and time to peak may be expressed as functions of the dimensionless parameter (as shown in equations (14) and (15)). These functions are shown graphically in figure 3.

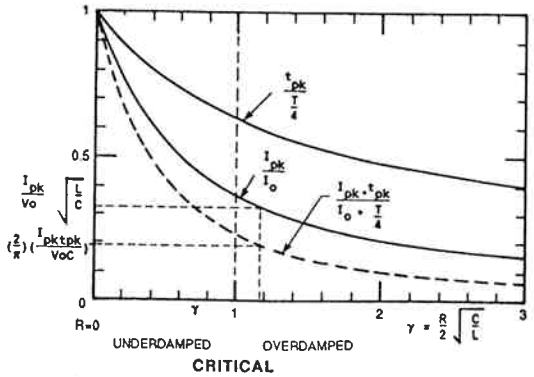


Figure 3. Variations of $I_{pk}$ and $t_{pk}$ as functions of the parameter γ

$$\frac{t_{pk}}{(\frac{T}{4})} = \frac{2}{\pi} \cdot \frac{\ln(\gamma + \sqrt{\gamma^2 - 1})}{\sqrt{\gamma^2 - 1}} \qquad (14)$$

$$\frac{I_{pk}}{I_o} = \left[\gamma + \sqrt{\gamma^2 - 1}\right]^{-\frac{\gamma}{\sqrt{\gamma^2 - 1}}} \qquad (15)$$

The product of equations (14) and (15) is shown as a dashed line in figure 3. The values of $I_{pk}$, $V_o$, $\omega_o$ and $t_{pk}$ are readily determined from the experimental data. The value of C can be readily calculated from equation (7). These parameters are combined to give an ordinate on the product curve which in turn establishes a value for $\gamma$. Projection of this point up onto the normalized current curve $I_{pk}/I_o$ defines the unknown value of L. Substituting known values into equation (13) allows for the calculation of the equivalent circuit resistance.

## Determination of Circuit Parameters
## Experimental Analysis

The value calculated for $R_{eq}$ (as shown in Table 1) by way of classical analysis compare favorably with the value determined through experimental methods. Application of Ohms Law allows for the determination of $R_{eq}$ in two steps.

First, the value of $R_1$ was calculated by taking the difference between the internal generated voltage of the machine, $V_{emf}$, and the instrument brush voltage $V_1$ at the time of peak current. Under the assumption that the excitation flux is constant.

$$V_{emf} = V_o\left(\frac{\omega_p}{\omega_o}\right) \qquad (16)$$

where $\omega_p$ is the value of rotor speed at the time of peak current.

Then,

$$R_1 = \frac{(V_{emf} - V_1)}{I(t_{pk})} \qquad (17)$$

Second, as can be seen in figure 2 the difference in the measured values of $V_1(t_{pk})$ and $V_2(t_{pk})$ divided by the peak current will yield the value of $R_2 + R_3$.

$$R_{eq} = R_1 + R_2 + R_3 \qquad (18)$$

Contained within the $R_2 + R_3$ measurement is the resistance drop of the sliding electrical contact. The resistance of the sliding interface is a function of current, surface speed, and contact pressure. For the majority of the discharge pulse, it is a relatively flat, slow changing function. For this reason the sliding interface resistance is also treated as a lumped element. For a more rigorous treatment of the interface the references [2, ..., 8] should be consulted.

## Instrumentation and Calibration

The ability to accurately assess the power supply circuit impedance is predicated upon the accuracy of the instrumentation used. Calibrated reference sources were used to establish base line values for the signals measured in this analysis. These reference sources include a precision current viewing resistor (CVR) and voltage supply.

The CVR was used to calibrate the Rogowski coil in place. In contrast to methods used in the past, calibration in place accounts for any localized magnetic field anomalies peculiar to the particular Rogowski/bus bar orientation. Figure 4. illustrates typical CVR and Rogowski current traces. It is evident that these curves are well behaved and that the Rogowski system does provide an accurate mapping of current behavior. The CVR characteristics are as follows:

| | |
|---|---|
| Bandpass: | 140 kHz |
| Rise Time: | 2.6 μs |
| Resistance: | 20.15 μΩ |
| Inductance: | negligible |
| Capacitance: | negligible |
| $I^2t$ rating | $4.5 \times 10^{10}$ $A^2$-s |
| Weight | 275 lb |
| Dimensions | 18W x 9H x 24L in. |

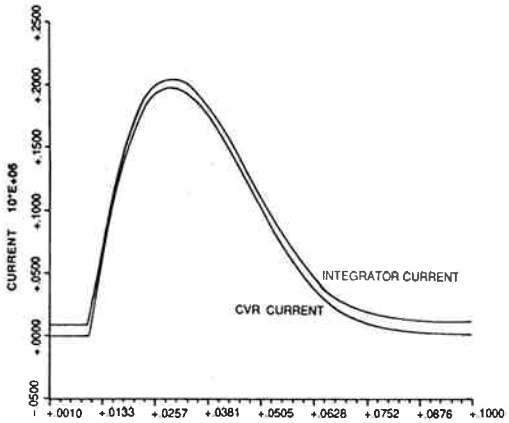


Figure 4. Typical CVR and integrated Rogowski current profiles

Three independent measurements of all signals were made. The measurement equipment utilized includes:

| Equipment | +/- Accuracy |
|---|---|
| Nicolet digital storage scope | 1/4096 of reading |
| CAMAC/Transiac digital recorder | 1/4096 of reading |
| CAMAC/Lecroy rotor speed scaler | $(RPM^2)/2E6$ |
| Honeywell Lightbeam Oscillograph | 5% of full scale |

Figure 5 illustrates a typical HPG discharge into the 56 μΩ, 225 nH loop resistor. Illustrating the instrument brush voltage, bus riser voltage rotor speed and discharge current. The reliability of the data is confirmed through the use of energy balance analysis.

Energy balance analysis equates the electromagnetic conversion energy to that of the mechanical energy of rotor rotation. Equation (19) expresses the relation between the two quantities. The summations are performed from time = 0 just prior to initial current flow.

$$\text{Total Energy} = \Sigma V_1(t)I(t)\Delta t + \Upsilon_m\Sigma\omega(t)\Delta t + R_1\Sigma I^2(t)\Delta t \qquad (19)$$

$\Upsilon_m$ is the mechanical torque due only to the friction drag of the sliding interface (brushes), J is the polar moment of inertia of the rotor, $\omega$ is the rotor speed, and the other parameters are detailed in Figure 2. Table 2 shows that $\Upsilon_m$ dominates in comparison to the other parasitic mechanical losses of windage, bearing, and seal losses. For the data in Table 1 the

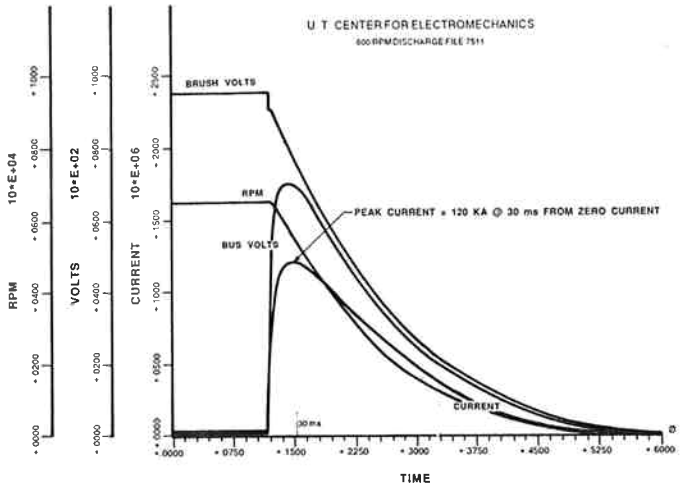


Figure 5. Typical discharge, 56 μΩ, 225 nH stainless steel load resistor

total energy was 110,300 J and the three terms on the right of equation 18 were 93,427, 12,168, and 5,180 J respectively. This indicates an energy balance to within 0.4 percent.

Table 2. Relative horsepower chart
Loss table (horsepower at 419 rad/s)

| Electromechanical Conversion | Bearing | Windage | Seal | $\Upsilon_m$ |
|---|---|---|---|---|
| $57 \times 10^3$ | 20 | 2 | 3 | 1,072 |

Future Parameter Modeling Considerations

The circuit model presented in Figure 2 is a lumped parameter model which does not include the adverse effects due to armature reaction and magnetic diffusion on the values of $R_{eq}$, $L_{eq}$, and $C_{eq}$. These effects will be the subject of a future study. They are defined here briefly only to point out that the effect of armature reaction on field flux increases the value of $C_{eq}$ in equation (4) and that the effect of magnetic diffusion skin depth increases the effective conductor cross sectional area as seen by the discharge current, thereby lowering the value of $R_{eq}$ (18). Both of these effects tend to increase as the load inductance since a large L will tend to increase the time to reach peak current. As was determined from the experiment data, the initial value of field flux was unchanged due to the short pulse duration.

Armature reaction results from the axial current which flows across the steel rotor during the discharge. This current produces a circumferential magnetic field in the rotor steel. The effect of this field models as a reluctance change in the magnetic circuit as seen by the excitation magnetic field. The net result is for the excitation field flux to decrease due to the increased magnetic circuit reluctance thereby resulting in a reduction of internal generator voltage ($V_{emf}$) and consequently of the discharge current.

Magnetic diffusion of the transient current pulse into the conductors causes the effective circuit resistance ($R_{eq}$) to vary with pulse length. The inability of the magnetic flux distribution within the conductors to change instantaneously results in the generation of eddy currents within the conductors as the transport current begins to rise. As these induced currents decay resistively, the transport current penetrates into the conductor, reducing the effective resistance of the conductor until the dc resistance is reached.

## Conclusions

Initial check out and characterization of the Balcones 60 MJ power supply has begun. Great care has been given to instrumentation, calibration, data retrival, and archiving. A simple lumped element circuit model for the generators has been rpesented and is adequate for first order system simulation. The Balcones system is a versatile high energy power source capable of driving a wide variety of pulsed power experiments. The data analysis system is capable of accurately recording experiments and verifying results. This unique assembly of capabilities will support the research efforts leading to the next generation of pulsed power development.

## References

[1] Heinz Knoepfel, ibid. p. 133: Pulsed High Magnetic Fields, North Holland Publishing Co, 1970.

[2] D. J. Ortloff, "The Design of a Brush Test Machine and the Verification of the Machine Design and Brush Design Under Test Conditions of High Current Densities and High Relative Surface Velocities," 1975.

[3] J. M. Weldon, "Design of a High Speed Controlled ATmosphere Test System for Sliding Electrical Contacts Conducting Large Power Pulses," 1976.

[4] J. M. Casstevens, "Measurement for the Friction and Wear Characteristics of Copper Graphite Sliding Electrical Contact Materials at Very High Speeds and Current Densities," 1976.

[5] M. J. Bharucha, "Testing and Evaluation of Brushes Used for the Fast Discharge Homopolar Generator Through the Use of the Controlled Atmosphere Brush-Testing Facility," 1978.

[6] M. Brennan, "The Experimental Investigation of the Effects of Contact Area and Large Currents on Sliding Electrical Contacts," 1979.

[7] R. A. Marshall, "Preliminary Results Obtained with a 400-kA Brush Tester," 1979.

[8] W. A. Walls, "Development of Actively Cooled Copper Brushes for High Performance Pulsed Homopolar Generator," 1985.